



System errors quantitative analysis of sample-scanning AFM

Xiaojun Tian^{a,b,c,*}, Ning Xi^{a,d}, Zaili Dong^a, Yuechao Wang^a

^aShenyang Institute of Automation, Academy of Sciences, Shenyang 110016, China

^bLiaoning Institute of Technology, Jinzhou 121000, China

^cGraduate School, Academy of Sciences, Beijing 100039, China

^dDepartment of Electrical and Computer Engineering, Michigan State University, East Lansing, MI 48824, USA

Received 27 May 2004; received in revised form 30 April 2005

Abstract

During imaging or nanomanipulation with a sample-scanning AFM, two important errors, scanning size error and vertical cross coupling error, will be generated due to bend motion of the tube scanner, and these two errors are destructive to nanostructures quantitative analysis. To minimize the errors, a kinematics model of the scanner is presented, and according to the model the two errors are quantitatively analyzed, which shows that scanning size error is greatly affected by sample thickness and nominal scanning size, while vertical cross coupling error is greatly affected by probe tip offset to tube axis and nominal scanning size. Corresponding methods are proposed for minimizing the errors. Gratings imaging experiments verify the kinematics model and errors calculation formulas.

© 2005 Elsevier B.V. All rights reserved.

PACS: 68.37.Ps; 06.20.Dk; 42.79.Ls

Keywords: Sample-scanning AFM; Tube scanner; Kinematics model; Scanning size error; Vertical cross coupling error

1. Introduction

Since the invention of atomic force microscope (AFM) by Binnig in 1986 [1], it has been a standard tool for imaging samples on a nanometer

scale. Recently, it has not only been used in characterizing nanostructures, it has been used in nanomanipulation [2–4]. Generally, AFM includes sample-scanning mode AFM, which means scanner actuates sample moving while probe keeps still, and tip-scanning mode AFM, vice versa. Single tube scanner is generally used in AFM [5]. The common structure of a single tube scanner in sample-scanning AFM is shown in Fig. 1. The main part of the tube scanner is a piezoceramics tube with one end attached to the sample stage,

*Corresponding author at: Shenyang Institute of Automation, Academy of Sciences, Shenyang 110016, China. Tel.: +86 24 23970540; fax: +8624 239 70021.

E-mail addresses: xjtian@sia.cn, hbtj@sina.com.cn (X. Tian).

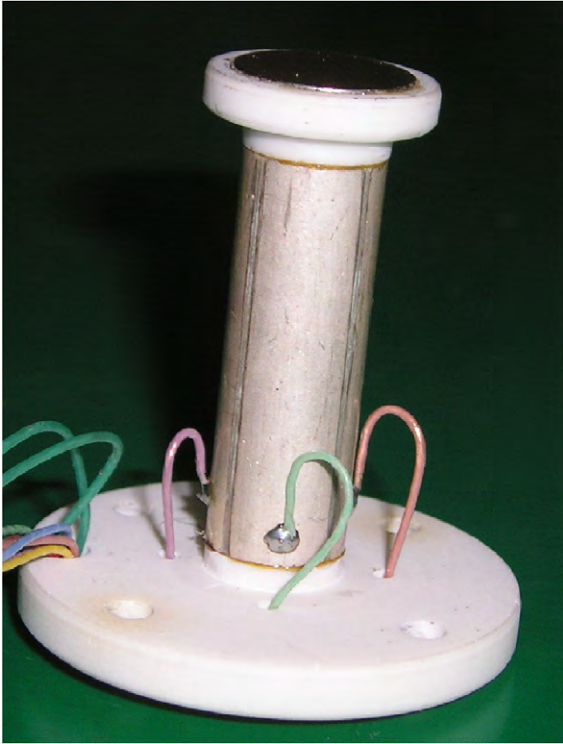


Fig. 1. Single tube scanner of sample-scanning AFM.

which is the free end, and the other end is fixed on a base. The inside and outside of the tube are plated with metal, and the outside is quartered with two opposite electrodes used as one part. When an ambi-polar voltage is applied, the tube will bend to realize a lateral scanning displacement. When voltage is applied to the inside, the vertical displacement will be realized.

During imaging a sample with a sample-scanning AFM, two important errors, namely cross coupling error and scanning size error, will be generated due to bend motion of the tube scanner, and the two errors are destructive to both image and probe positioning accuracy in nanomanipulation. Many researches have been done on tube scanner errors caused by piezoceramics intrinsic characteristics such as nonlinearity and hysteresis, and various calibration and nonlinearity correction methods have also been proposed [6–9]. Some models mainly to investigate scanner dynamics have also been proposed, e.g., a complex dynamic

model considering the coupling between motions in different axes has been presented in Ref. [10] and a linear fifth-order model of the scanner lateral dynamics for open-loop control to enable fast imaging has been investigated [11]. While system errors quantitative analysis, to which kinematics modeling is indispensable, has seldom been done.

In this paper, kinematics model of the tube scanner is presented based on its motion analysis, scanning size error and cross coupling error according to the model are quantitatively analyzed for adopting corresponding methods to promote the accuracy in both imaging and nanomanipulation. Experimental results have verified the proposed model and errors calculation formulas.

2. Kinematics model of tube scanner

When ambi-polar voltage is applied on two opposite electrodes of scanner outside, the tube will bend as shown in Fig. 2, and sample will generate lateral translation and rotation relative to

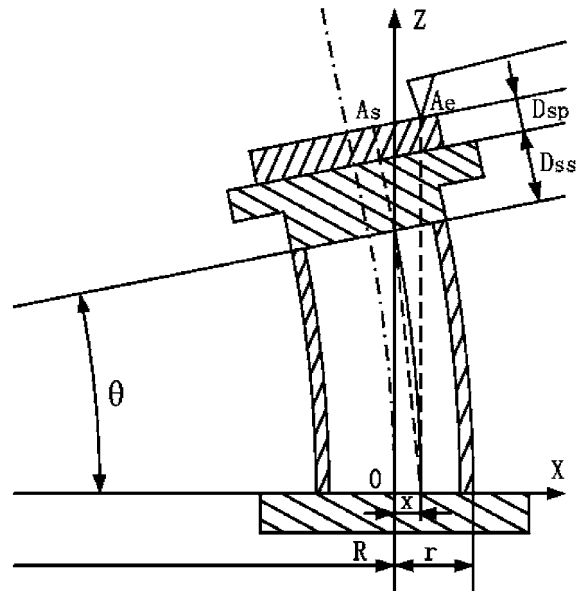


Fig. 2. Kinematics model of single tube scanner of sample-scanning AFM.

fixed probe, thus displacement of any point on the sample is different.

In Fig. 2, the part clipped by angle θ is a piezoceramics tube, the part pointed by Dss is the sample stage, and Dsp means the sample.

Supposing the material of the scanner is uniform and its structure is symmetric, and scanner axis is viewed as the symmetric axis, the extension and condensation will be the same with ambi-polar voltage applied to the two opposite electrodes and the bend geometry can be viewed as a circular arc [12]. We have

$$(R + r)\theta = L + \Delta L, \quad (R - r)\theta = L - \Delta L, \quad (1)$$

where r is the outside radius of the tube, R is the curvature radius of the tube axis, θ is the central angle, L is the initial length of tube and ΔL is the extension of the tube after a voltage is applied to the tube outside.

The extension of the tube can be presented [13] as

$$\Delta L = Ed_{31}L = \frac{d_{31}L}{t}U_x, \quad (2)$$

where E is the electric field intensity along tube wall, U_x is the voltage along x -axis, t is the thickness of the tube wall and d_{31} is the piezoelectric constant along the tube axis.

Substituting Eq. (2) into Eq. (1), one can obtain the expression of θ :

$$\theta = \frac{L}{R} = \frac{d_{31}L}{tr}U_x. \quad (3)$$

Before the tube bends, the lateral coordinate of the point on the sample, corresponding to the probe tip offset to the tube axis, is x and vertical coordinate of the point is $L + D_{ss} + D_{sp}$. After the tube bends to the left as shown in Fig. 2, the point moves to point As, then the displacement of the scanner (or the point on sample) can be presented as

$$\begin{aligned} dx &= (R + x)(1 - \cos \theta) + (D_{ss} + D_{sp}) \sin \theta, \\ dz &= ((R + x) \sin \theta - L) + (D_{ss} + D_{sp})(\cos \theta - 1). \end{aligned} \quad (4)$$

When the tube extends, tube wall thickness will reduce and the change will be $\Delta t = d_{33}U_x$ [13], where d_{33} is the piezoelectric constant vertical to

the tube axis. d_{33} is on sub-nanometer per voltage scale [13], and generally U_x is below one 1000 v, Δt is on sub-micrometer scale, and compared with t on millimeter scale, Δt can be ignored and t can be viewed as a constant.

Thus if t , r , L and d_{31} are all constants for a given scanner, then θ and R only depend on U_x according to Eq. (3), and as Dss is also a constant, the lateral and vertical displacements (dx and dz) at any point on the sample depend on applied voltage U_x , its offset to the tube axis x and the sample thickness Dsp.

3. Scanning size error and vertical cross coupling error

As shown in Fig. 2, the lateral position of the probe tip contacting the point on the sample, corresponding to the center of the scanning area on the sample, is decided by its offset to the tube scanner axis, which can be adjusted manually by adjusting the tube scanner base position before imaging starts.

After tube bending, shown in Fig. 2, the sample's point touched by the probe tip has changed from point As to point Ae, and point Ae's vertical coordinate z_{Ae} is

$$z_{Ae} = (R + x) \tan \theta + (D_{ss} + D_{sp}) / \cos \theta. \quad (5)$$

Thus the right scanning area covers the area from point Ae to point As, and its size Lrss can be obtained as

$$\begin{aligned} L_{rss} &= ((R + x)(1 - \cos \theta) \\ &+ (D_{ss} + D_{sp}) \sin \theta) / \cos \theta. \end{aligned} \quad (6)$$

Likewise, when the tube bends right, the size of the left scanning area Llss can also be obtained as

$$\begin{aligned} L_{lss} &= ((R - x)(1 - \cos \theta) \\ &+ (D_{ss} + D_{sp}) \sin \theta) / \cos \theta. \end{aligned} \quad (7)$$

Then the whole scanning size Lss can be deduced from Eqs. (6) and (7)

$$L_{ss} = 2(R(1 - \cos \theta) + (D_{ss} + D_{sp}) \sin \theta) / \cos \theta. \quad (8)$$

If D_{ss} is a constant and θ or R only depend on U_x , the scanning size depends on U_x and D_{sp} .

3.1. Scanning size error

AFM is calibrated before sample-scanning, the thickness of the grating used in lateral calibration can be called nominal sample thickness D_{nsp} , after calibration the scanning size can be called nominal scanning size L_{nss} , which is a pointed value on the scanning program interface and can be easily changed by the user, and it can be obtained from Eq. (8) as

$$L_{nss} = 2(R(1 - \cos \theta) + (D_{ss} + D_{nsp}) \sin \theta) / \cos \theta. \quad (9)$$

If D_{nsp} is a constant, and θ and R only depend on U_x , L_{nss} also depends only on U_x , which means that L_{nss} is corresponding to θ or R .

When sample thickness is not equal to the nominal one, there will be an error between actual scanning size and nominal one. From Eqs. (8) and (9), scanning size error dL_{ss} can be presented as

$$dL_{ss} = 2(D_{sp} - D_{nsp}) \tan \theta. \quad (10)$$

If D_{nsp} is a constant, dL_{ss} depends on D_{sp} and θ that corresponds to L_{nss} , and the simulation result of scanning size error dL_{ss} dependence on sample thickness D_{sp} and nominal scanning size L_{nss} is shown in Fig. 3.

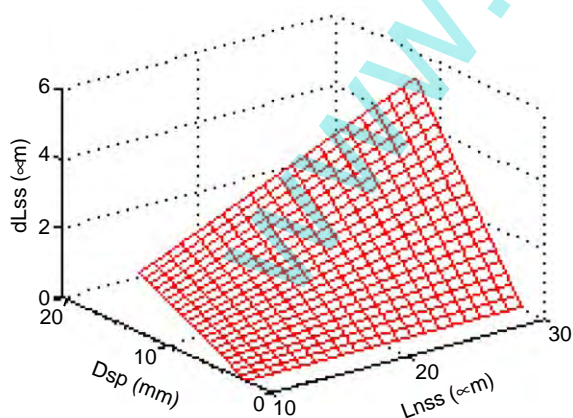


Fig. 3. Simulated dependent curve of scanning size error on sample thickness and nominal scanning size (while nominal sample thickness is 2 mm with tube length 52 mm and sample stage thickness 4 mm).

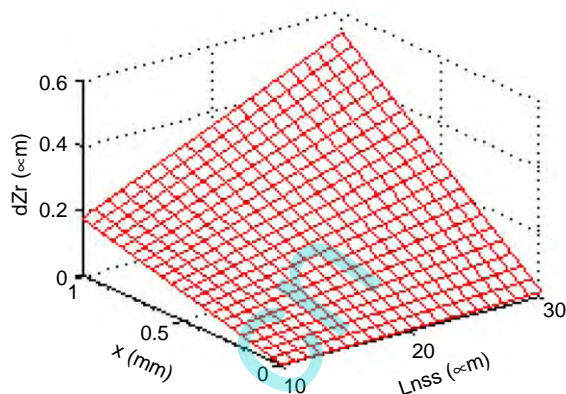


Fig. 4. Simulated dependent curve of vertical cross coupling error on its offset to tube axes and nominal scanning size (while sample thickness keeps 2 mm with tube length 52 mm and sample stage thickness 4 mm).

3.2. Vertical cross coupling error

After the tube bends to the left as shown in Fig. 2, the vertical cross coupling error dZ_r deduced from Eq. (5) is

$$dZ_r = (R + x) \tan \theta - L + (D_{ss} + D_{sp}) \times (1 / \cos \theta - 1). \quad (11)$$

If D_{ss} and L are constants, and θ or R corresponds to the nominal scanning size, it can be seen that the vertical cross coupling error dZ_r depends on its offset (also tip offset) to the tube axis x , nominal scanning size L_{nss} and sample thickness D_{sp} , the simulation result is shown in Fig. 4.

Specially, when the point's offset to the tube axis is zero and the sample thickness is equal to the nominal one, the simulated result of vertical cross coupling error dependence on nominal scanning size is shown in Fig. 5.

It can be seen that the error in Fig. 5 is very small compared with that in Fig. 4 especially when the scanning size is small, which means that the offset is a dominant factor causing vertical cross coupling error.

4. Experiment and verification

In order to verify the proposed model and error calculation formula, some imaging of gratings are performed.

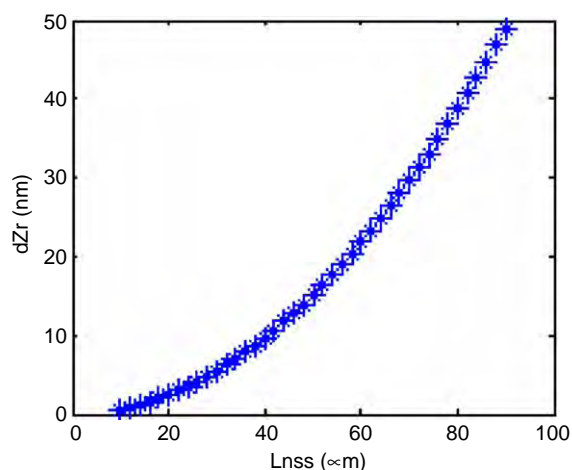


Fig. 5. Simulated dependent curve of vertical cross coupling error on nominal scanning size with offset equal to zero (while sample thickness is 2 mm with tube length 52 mm and sample stage thickness 4 mm).

4.1. System configuration

A sample-scanning AFM (model CSPM-2000wet, Ben Yuan Ltd., China) was used for imaging nanostructures or samples. A scanner is equipped in the AFM head with a maximum XY scan range of $30 \times 30 \mu\text{m}^2$ and a Z range of $3 \mu\text{m}$. Silicon nano-probe (MickoMasch Inc.) with V-shaped cantilevers is used. In order to facilitate imaging, an optical microscope and a CCD camera are also included in the system shown in Fig. 6.

In the system, the AFM head is controlled by a CSPM 2000 wet controller connected to the computer. The computer responds to running system control program and provides an interface for the user to change parameters in scanning samples. The optical microscope and CCD camera help the operator to adjust the laser to focus on the cantilever end and search for an interesting area on the sample.

4.2. Scanning size error and minimizing method

To a grating with $3 \mu\text{m}$ width's steps (MickoMasch Inc.), actual scanning size rises as grating thickness increasing, as shown in Fig. 7.



Fig. 6. The configuration of AFM based imaging system: (1) AFM control computer; (2) CSPM 2000wet controller; (3) AFM head; (4) optical microscope; (5) CCD camera; (6) monitor.

Adjusting the grating thickness, we can get the change table of scanning size as shown in Table 1.

From experiments we can conclude that experimental data are in accordance with the theoretical one. When sample thickness equals to the nominal one, the actual scanning size is equal to the nominal one. If the two ones are not the same, the actual scanning size will be greatly affected by sample thickness and the nominal one. Keeping the nominal scanning size constant, the actual one will increase with sample thickness increasing. So, for minimizing scanning size error in imaging nanostructures, we can firstly increase or decrease sample thickness to make it equal to the nominal one. To special sample whose thickness cannot be changed, we can compensate the scanning size error by Eq. (10).

4.3. Vertical cross coupling error and minimizing method

Before imaging, the sample will be actuated by a tube scanner to approach the probe tip and the tip

Table 1
Measured scanning size and theoretical one with sample thickness changing (nominal scanning size keeps 30 μm)

Sample thickness (mm)	Measured scanning size (μm)	Theoretical scanning size (μm)
2	30.0	30.000
4	31.0	31.034
6	31.9	32.068
8	33.2	33.103
10	34.1	34.137

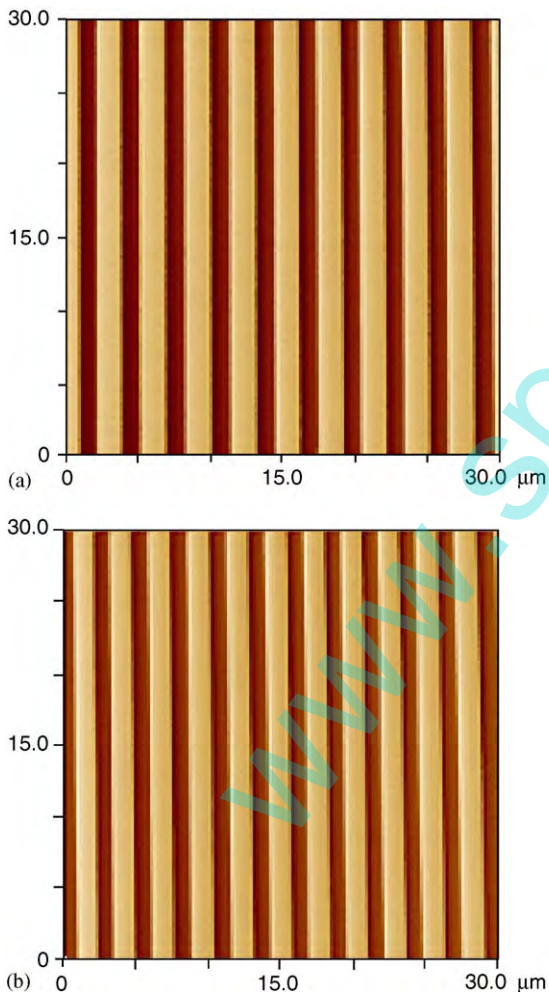


Fig. 7. Two scanning images of a grating with grating thickness 2 mm in image (a) and 10 mm in image (b) while nominal scanning size keeps 30 μm.

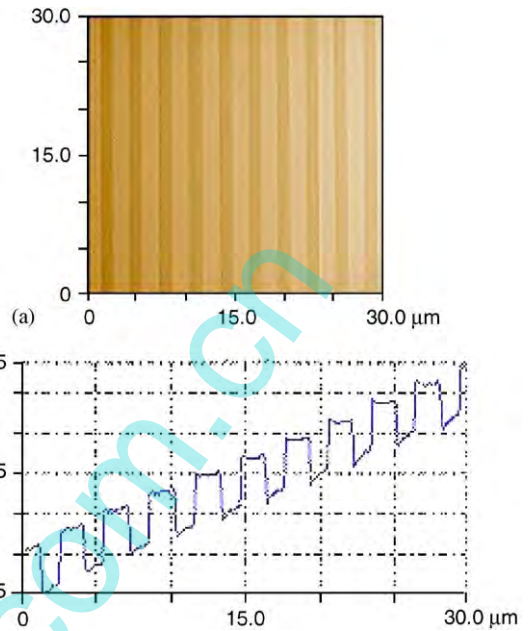


Fig. 8. Scanning image (a) and its cross section (b) of grating with tip offset equal to 0.5 mm when scanning size is 30 μm (Note that in the cross section image, the effect of hysteresis and creep is obvious, while the “bow” shape is not obvious for the effect of bow effect in vertical direction is very small compared with the effect mainly caused by the tip offset especially when the scanning size is small.).

will touch at a point on the sample, and the point, corresponding to the center of the scanning area is decided by tip offset to the scanner axis, as shown in Fig. 2, which can be adjusted manually by adjusting the tube scanner base position before imaging starts.

The height error of the grating step’s top surface is only 1.5 nm (Mikromasch Inc.), its surface can be considered as an even plane for measuring vertical cross coupling error as shown in Fig. 8.

Changing the tip offset when the nominal scanning size keeps 30 μm, we got the table of vertical cross coupling error changing as shown in Table 2.

Thus we can conclude that experimental data are in accordance with the theoretical one. When the tip offset is zero and scanning size is small, vertical cross coupling error is small. While tip offset is not zero, vertical cross coupling error will rise greatly with tip offset increasing.

Table 2
Vertical cross coupling error with tip offset changing from -0.5 mm to 0.5 mm (nominal scanning size keeps $30\ \mu\text{m}$)

Tip offset (mm)	Measured vertical cross coupling error (nm)	Theoretical vertical cross coupling error (nm)
-0.5	-261	-253
-0.25	-119	-124
0	9	5
$+0.25$	130	134
$+0.5$	250	263

Although vertical cross coupling error in imaging caused by tip offset can be minimized by post-imaging correction method, it will still exist in nanomanipulation with a sample-scanning AFM system and must be minimized for improving nanomanipulation accuracy. For minimizing vertical cross coupling error in nanomanipulation, tip offset to tube axis can be firstly reduced to zero by adjusting the tube scanner base position, while on those occasions where tip offset cannot be adjusted to zero, we can compensate it in the trajectory planning of nanomanipulation according to the error calculation formula shown as Eq. (11).

5. Conclusion and outlook

Scanning size error and cross coupling error greatly affects the accuracy of imaging and nanomanipulation with a sample-scanning AFM. With scanning size error and cross coupling errors quantitatively analyzed according to the kinematics model presented in this paper, some methods are proposed to minimize the errors, thus the accuracy in imaging and manipulation can be significantly enhanced.

Based on the kinematics modeling and errors analyzing work described above, in the next step we will build a sample-scanning AFM-based

nanomanipulation system with high positioning accuracy of the AFM probe and also real-time forces and visual feedback during manipulation, by which we expect to do some research work on manipulating and assembling nanowires or nanotubes and eventually fabricate nanoelectronic devices such as nanosensors, nanotransistor, etc.

Acknowledgments

The authors would like to thank the financial support from NHTRDP (863 Program), P.R China (Nos. 2002AA422210 and 2003AA404070). Here we also thank the reviewers for their comments and suggestions.

References

- [1] G. Binnig, C.F. Quate, C. Gerber, *Phys. Rev. Lett.* 56 (9) (1986) 930.
- [2] R. Luthi, E. Meyer, H. Haefke, L. Howald, W. Gutmannsbauer, H.J. Guntherodt, *Science* 266 (1994) 1979.
- [3] D.M. Schaefer, R. Reifenberger, A. Patil, R.P. Andres, *Appl. Phys. Lett.* 66 (1995) 1012.
- [4] T. Junno, K. Deppert, L. Montelius, L. Samuelson, *Appl. Phys. Lett.* 66 (26) (1995) 3627.
- [5] G. Binnig, D.P.E. Smith, *Rev. Sci. Instr.* 57 (8) (1986) 1688.
- [6] J.F. Jørgensen, L.L. Madsen, J. Garnæs, K. Carneiro, K. Schaumburg, *J. Vac. Sci. Technol. B* 12 (3) (1994) 1698.
- [7] R. Durselen, U. Grunewald, W. Preuss, *J. Scan. Microsc.* 17 (2) (1995) 91.
- [8] S. Ito, *Proceedings of the SICE Annual Conference*, 1994, p. 927.
- [9] J. Akila, S.S. Wadhwa, *Rev. Sci. Instr.* 66 (3) (1995) 2517.
- [10] O.M. E. Rifai, K.Y. Toumi, *Proceedings of American Cont. Conference* 4 (2001) 3251.
- [11] G. Schitter, A. Stemmer, *Microelectron. Eng.* 67 (2003) 938.
- [12] C. Wei, H.H. Zhang, L. Tao, W.J. Li, H.M. Shi, *Rev. Sci. Instr.* 67 (6) (1996) 2286.
- [13] J.A. Gallego-Juarez, *J. Phys. E.* 22 (1989) 804.